Theoretical Studies on the Conformational Change of Adenosine Kinase Induced by Inhibitors

LIHUA DONG,[1,2,3] JUNYOU SHI,[1,3] JINHU WANG,[4] YONGJUN LIU[1,4]

[1]*Northwest Institute of Plateau Biology, Chinese Academy of Sciences, Xining, Qinghai 810001, China*

[2]*School of Chemistry and Chemical Engineering, Taishan Medical University, Taian, Shandong 271000, China*

[3]*Graduate University of Chinese Academy of Science, Beijing 100049, China*

[4]*School of Chemistry and Chemical Engineering, Shandong University, Jinan, Shandong 250100, China*

Received 1 August 2010; accepted 20 August 2010
Published online 30 November 2010 in Wiley Online Library (wileyonlinelibrary.com).
DOI 10.1002/qua.22939

ABSTRACT: Adenosine kinase (AK) is a two-domain protein that catalyzes the phosphorylation of adenosine to adenosine monophosphate. Inhibitors of AK could increase adenosine to levels that activate nearby adenosine receptors and produce a wide variety of therapeutically beneficial activities. To get insight into the interaction mechanism between inhibitors and AK, we chose two kinds of novel inhibitors, alkynylpyrimidine inhibitor (APy) and aryl-nucleoside inhibitor (AN), and used docking and molecular dynamics simulation methods to study the conformational changes of human AK on binding inhibitors. The calculation results revealed that both APy and AN could induce conformational changes of AK and stabilize AK at different semiopen conformations. On binding APy, the small lid-domain rotated 14°, and the binding pocket rearranged after MD simulation. But in AK-AN complex, the rotation of small domain is 22°, and the sugar ring of AN is mobile in the binding pocket. Further docking calculations on APy analogues indicate that the semiopen conformation could well explain the SAR of AK inhibitors. Int J Quantum Chem 111: 3980–3990, 2011

Key words: adenosine kinase (AK); inhibitor; conformational change; molecular dynamic (MD)

Correspondence to: Y. Liu; e-mail: yongjunliu_1@sdu.edu.cn

Additional Supporting Information may be found in the online version of this article.

1. Introduction

Adenosine (ADO) is an important endogenous neuromodulator that functions as an extracellular signaling molecule within the central nervous system and peripheral nervous system [1, 2]. Under conditions of metabolic stress and trauma (including ischemia, seizures, inflammation, and pain), extracelluar concentrations of ADO are increased and act to limit tissue damage and restore normal function by activating members of the P1 receptor family, A_1, A_{1A}, A_{2B}, and A_3 receptors [2]. However, because ADO has short half-life time on the order of seconds in physiological fluids [3], its extracellular actions are restricted to the tissue and cellular sites where it is released. The effects of the extracellular ADO are terminated by its reuptake and metabolization by some ADO-metabolizing enzymes [4].

Among all the ADO-metabolizing enzymes, adenosine kinase (AK) is the first enzyme that catalyzes the phosphorylation of ADO to AMP and, therefore, is a key enzyme in controlling the cellular concentrations of ADO. Because the transport of ADO across the cellular membrane is diffusive and equilibratory [5], the inhibition of AK, by preventing ADO phosphorylation, results in the accumulation of intracellular ADO, which in turn leads to a net release of ADO to the extracellular compartment [6]. Consequently, AK inhibitor can enhance the endogenous protective action of ADO. It is reported that AK inhibitors have been shown to demonstrate potential clinical utility in animal models of epilepsy, ischemia, pain, convulsion, and inflammation [7–11].

Up to now, numbers of AK inhibitors have been identified and synthesized, which can be divided into two classes. One is nucleoside inhibitors, including 5′-deoxy-5′-amino-ADO [12], 5′-deoxy-5-iodotubercidin [13], clitocine [14], GP-3269 [15] etc., which have structural resemblance to the natural ligand ADO; the other is non-nucleoside inhibitors, such as pyridopyrimidine analogues [16] or alkynylpyrimidine analogues [17], which have been synthesized mainly by Abbott Laboratories and proved having potent inhibitory activity [17–21].

The AK enzyme is a member of the ribokinase enzyme family. The structure of human AK in complex with ADO [22] has been reported as well as structures of *Toxoplasma gondii* AK and *Mycobacterium tuberculosis* AK both in the apo (apoenzyme) form and in complex with inhibitors [23–26]. AK is a two-domain protein as shown in Figure 1, the ADO binding site locates at the interface of the large and small domains, whereas the cofactor ATP binds at an adjacent site in the large domain. Like other ribokinase family members, AK undergoes large conformational changes on ligand binding. It had been assumed that all inhibitors bound to AK in a manner analogous to ADO in both the binding interactions and protein conformations [27, 28]. However, recently, it has been found [29] that nucleoside and non-nucleoside inhibitors bound to AK in two different modes, namely closed and open conformations, respectively. Furthermore, Bhutoria and Ghoshal [30] proposed that the structural diverse nucleoside inhibitors could bind to AK in different fashion. Based on the degree of substitutions at C4 and C5 positions, nucleosides were divided into aryl and nonaryl nucleoside inhibitors. By using docking analysis and homology modeling, Bhutoria and Ghoshal concluded that the aryl nucleoside analogues could bind to the semiopen conformation of human AK, whereas the nonaryl nucleosides bind to the closed conformation.

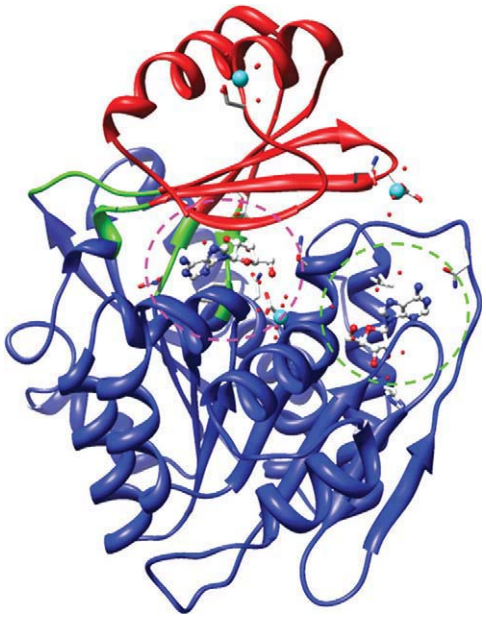

FIGURE 1. The crystal structure of human AK complexed with ADO (PDB code 1BX4). The small domain is shown in red and the large domain in blue. These two domains are connected by four peptide segments (R14-16, 62-65, 117-121, 138-141), which are shown in green. The pink and green elliptical parts represent ADO and ATP binding sites, respectively. [Color figure can be viewed in the online issue, which is available at wileyonlinelibrary.com.]

Although several crystal structures of AK complexed with inhibitors have been obtained, the

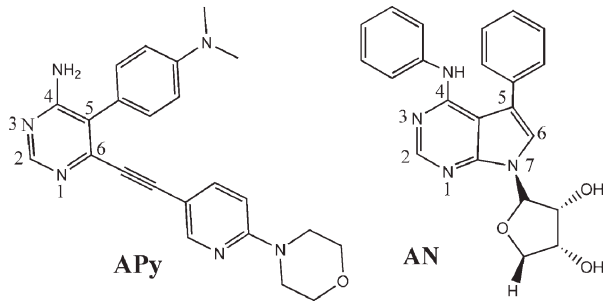

FIGURE 2. Structure of APy and AN.

reason why different inhibitors bind to AK in different conformations as experimentally achieved is still unclear. The theoretical research on AK inhibitors is limited to the DOCK and QSAR (quantitative structure-activity relationship) studies, while the ligand-induced conformational changes have been ignored. In this study, we chose two representative inhibitors: an alkynylpyrimidine inhibitor (APy) [29] and an aryl-nucleoside inhibitor (AN) [31] (see Fig. 2), used docking and molecular dynamics simulation methods to study the conformational changes of human AK on binding ligands, and explained the interactions between AK and inhibitors.

2. METHODS

Because the crystal structure of human AK apo has not been obtained, considering that *T. gondii* AK (TAK) apo and *M. tuberculosis* AK apo are open conformations, we conjecture that human AK apo may also adopt its open conformation. The crystal structure of human AK complexed with inhibitor APy (PDB code 2I6B) was used to represent the open conformation of AK. This structure contains two chains: chain A and chain B, the former was used in the docking experiments. In this system, ligands and crystallographic waters not hydrogen bonded with AK were deleted, and then, the incomplete residues in AK were repaired, but the missing residues were not added because they are far from the active site and do not appear to affect the function of AK.

The inhibitors APy and AN were fully optimized at the level of 6-31G(d) by using the Becke-3-parameter-Lee-Yang-Parr (B3LYP) hybrid density functional theory with Gaussian 03 package [32].

2.1. AUTOMATED DOCKING SETUP

Docking was performed with version 4.0 of the program AutoDock [33, 34]. When docking, AK was kept rigid, whereas all the torsional bonds of each ligand were set free. The dimensions of the grids were set as 60 × 60 × 60 based on grid module, with a spacing of 0.375 Å between the grid points. Polar hydrogen atoms and Kollman United Atom Charges were added to the receptor. Fifty independent docking runs were performed for each ligand. Based on a root-mean-square deviation (RMSD) criterion of 0.1 nm, the docking results were clustered.

2.2. MOLECULAR DYNAMICS SETUP

Molecular dynamics simulations of AK complexed with inhibitors APy and AN were performed by GROMACS program [35]; ligands APy and AN were parameterized by PRODRG server [36]. In the calculation, each complex was placed in the center of a 70 Å × 70 Å × 70 Å cubic box and solvated by SPC216 water molecules. Five Na^+ counter ions were added to satisfy the electroneutrality condition. Berendsen temperature coupling and Berendsen pressure coupling were used to keep the system in stable environment (300 K, 1 Bar); the coupling constants were set to 0.1 ps. The particle mesh Ewald algorithm was used to calculate long-range electrostatic interactions with a cutoff of 1.0 nm. The cutoff value for van der Waals and neighbor list interactions were set to 1.2 nm, and the LINCS algorithm for bond constrains was applied. Each complex was energy minimized for 5,000 steps of steepest descents, following with a 200-ps position restraining simulation. Finally, the restraints were removed, and the 20-ns MD simulations were performed.

3. Results and Discussions

3.1. DOCKING

The docking results of APy and AN to the open conformation of AK are shown in Figure 3, in which both ligands lay in the same binding cavity formed at the interface of the large and small domain of AK. The binding energies calculated by docking for APy and AN are −6.86 and −10.07 kcal/mol, respectively, which is in accordance with their experimental IC_{50} values, 68 nM for APy [29] and 0.5 nM for AN [31].

For APy [Fig. 3(a)], the binding pocket consists of residues N14, L40, S65, L138, F170, and F201. The pyrimidine ring of APy forms a stacking interaction with the phenyl group of F170. N3 atom in the pyrimidine ring makes two H-bonds with the main-chain nitrogen atom and side-chain

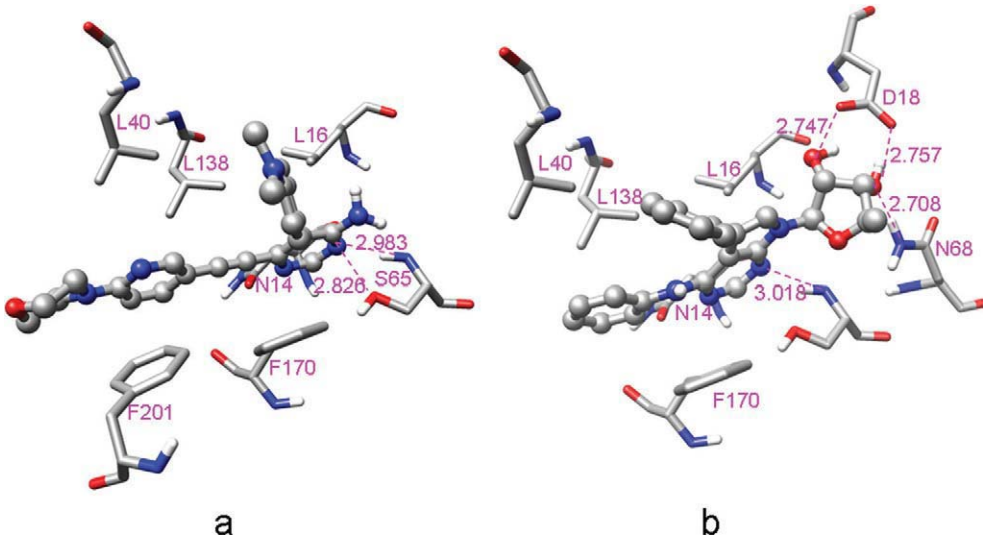

FIGURE 3. Docking structures of open AK with inhibitors APy (a) and AN (b). Only the residues within 0.5 nm are shown. In each structure, the magenta dotted lines represent hydrogen bonds (unit: 0.1 nm). [Color figure can be viewed in the online issue, which is available at wileyonlinelibrary.com.]

hydroxyl of S65. The pyridine ring and acetylenic linker of APy are sandwiched between the hydrophobic residues L40 and L138 in the small domain and residues F170 and F201 in the large domain. The morpholine ring is exposed to solvent. The docking result of APy agrees well with the crystal structure [29], suggesting our docking calculations are reliable.

Figure 3(b) shows the interaction details of AN with the protein. Residues N14, L16, L40, S65, L138, F170, D18, and N68 compose the binding pocket. There is stacking interaction between the purine base and the phenyl group of F170. N1 atom in purine base forms one H-bond with the main-chain nitrogen atom of S65. Exocyclic hydroxyls of the sugar ring form two H-bonds with the side-chain oxygen atoms of D18 and one H-bond with the side-chain nitrogen atom of N68.

Comparing the docking results of these two ligands, we can see that there are some similar binding modes between APy and AN, despite their structural difference. First, the pyrimidine rings of both ligands make direct interaction with residues S65. Second, the phenylamine substituent at C4 position of AN adopts the same orientation as the pyridine ring of APy. Third, both the nonpolar substituents at C5 position of AN and APy extend to the same hydrophobic pocket formed by residues L16, A136, and L138.

Furthermore, because AN is an aryl nucleoside inhibitor, we compared its docking result with the crystal structure of 2I6A (a nonaryl nucleoside inhibitor 5I5 binding to the closed conformation of AK). From Figure 4, we can see that the interactions of these two ligands with the protein are similar. The only difference is the H-bond between 5I5 and the side chain of residues N14, which is not found in docking result of AN. The earlier docking results reveal that AN combined the binding modes of both APy and ADO, which made it binds tightly to the protein.

3.2. MOLECULAR DYNAMICS SIMULATIONS

Based on the docking conformations, molecular dynamics simulations were performed to investigate the conformational changes of AK after binding APy and AN. For comparison, we also performed MD simulation on 2I6B apo structure (open conformation of AK without ligand) to study its kinetic characteristics. The RMSDs of these systems are shown in Figure 5. The RMSDs of AK relative to itself reflect the structural stability of protein, and the RMSDs of ligand relative to protein reveal the binding stability of the ligand. From Figure 5(a), we can see that these systems reached equilibrium within 20 ns, the RMSDs of protein relative to itself are as follows: 2I6B apo, 3.0 Å; AK-AN, 2.5 Å; and AK-APy, 2.0 Å. 2I6B apo system underwent the largest structural change, and AK-APy corresponded the smallest change. The RMSDs of the ligands

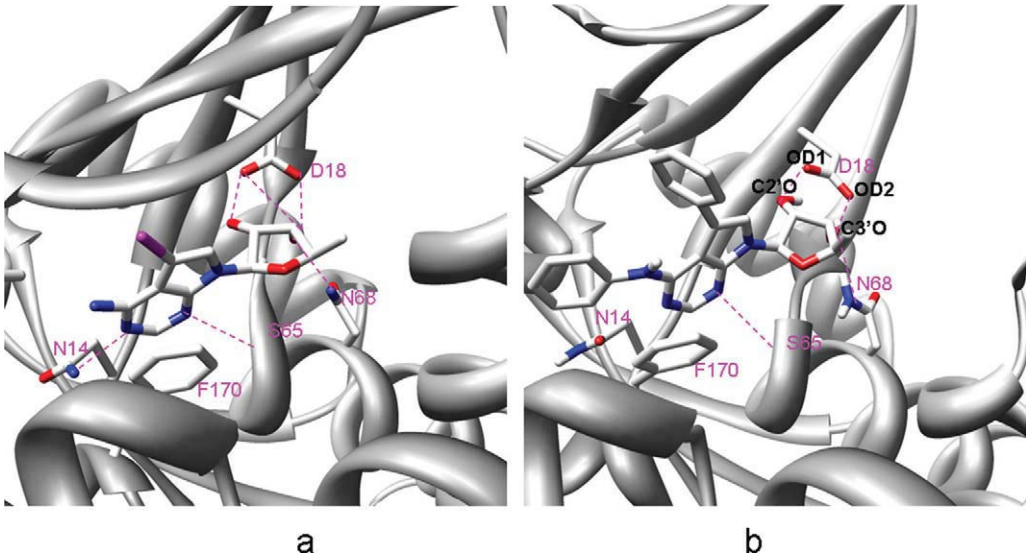

FIGURE 4. Comparison of the binding sites between crystal structure of 2I6A (a) and docking structure of AK-AN (b). [Color figure can be viewed in the online issue, which is available at wileyonlinelibrary.com.]

relative to AK [Fig. 5(b)] indicate that APy experienced a remarkable change compared with its original binding site and then stabilize at 5.0 Å, but inhibitor AN only changed slightly, which is in accordance with the docking results.

The time evolutions of the radius of gyration for the three systems are shown in Figure 6(a). Radius of gyration is indicative of the level of compaction in the structure. The initial radiuses of these three systems were the same. But after simulations, all of them decreased. For 2I6B apo, the radius changed from 19.6 to 18.7 Å in the initial 5 ns and, then, stabilized at ~18.8 Å. For AK-APy and AK-AN systems, they stabilized at ~19.3 and ~19.0 Å, respectively. It indicates that in the absence of ligands, 2I6B apo shrank into the most compact form. It also shows that inhibitors APy and AN made great influence on the conformational change of AK, which will be discussed in the following sections.

We also calculate the time evolution of the root mean square fluctuates (RMSF) from the averaged structure, which provides another approach to evaluate the convergence of the dynamical properties of the system. Figure 6(b) shows the atomic fluctuations averaged over residues for the three systems derived from the 20-ns MD trajectories. For comparison, the corresponding values of

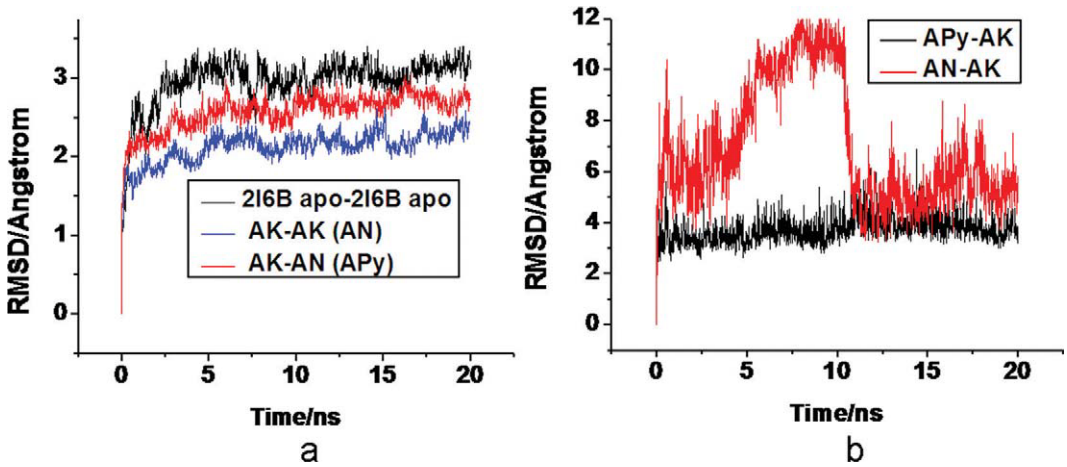

FIGURE 5. Time dependence of RMSDs: (a) AK relative to itself; (b) ligands to AK. [Color figure can be viewed in the online issue, which is available at wileyonlinelibrary.com.]

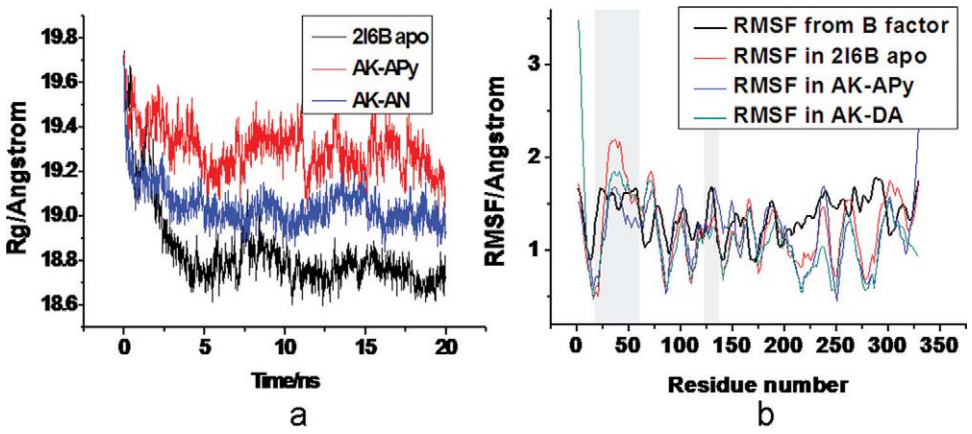

FIGURE 6. (a) Time evolution of radius of gyration for each system over three MD simulations. (b) Residues RMSF obtained from MD trajectories and from B factors. The highly flexible residues in the small domain are highlighted. [Color figure can be viewed in the online issue, which is available at wileyonlinelibrary.com.]

RMSF obtained from the experimental B factors in crystal structures of 2I6B are also shown. The experimental B factors are transformed to the crystallographic RMSF with the formula $\langle \Delta r^2 \rangle = 3B_i/(8\pi^2)$ [37]. RMSF profiles indicate that the small lid domain of AK (residues 17-61 and residues 122-137) has higher values, reflecting that the small domain made great fluctuant during the MD simulations. This is in agreement with the experimental B factors, indicating the reasonability of our MD results.

3.2.1. Conformational Change of AK Complexed With APy

Figure 7(a) shows the superposition of AK-APy complex from the docking and the final MD simulation.[1] The most striking feature in comparison with the two structures is a rigid-body motion of the small domain relative to the large domain. The rotation of the small domain is ~14° calculated by the program DYNDOM [38, 39]. The backbone RMSD of AK is 2.0 Å, and the conformation of AK stabilizes at a semiopen state.

Comparing with the docking results, we found that some residues in the binding pocket changed their position after MD simulation. First, the side chain of residue N14 rotated almost 180° and formed a stable H-bond with N1 atom of pyrimidine ring. Because N14 is a conserved residue in AK family, the H-bond between this residue and ligands can be seen in almost all of the AK complexes [22–25]. Next, in docking structure, the N3 atom of the pyrimidine ring formed two H-bonds with residue S65 [Fig. 7(b)]. During MD simulation, S65 twisted outward, and the corresponding H-bonds disappeared, then the pyrimidine ring of APy rotated toward the binding pocket and formed two H-bonds with the main and side chains of T66 [see Fig. 7(c)]. Furthermore, we also noted that the morpholine ring of APy was mobile during MD simulation, which is in accordance with the high B-factors for the atoms in that ring [29].

During MD simulation, residues 295–297 coiled and were prone to form helix. However, along with the small lid-domain rotating to the large domain, Q38 in the small domain moved down and formed one H-bond with the side chain of N296 [the elliptical part in Fig. 7(a)], which kept residues 295–297 maintain coil instead of helix.

To examine the rationality of the conformational change of AK after MD simulation, we chose five APy analogues (AP0-AP4 as shown in Fig. 8) and performed docking to the average structure of AK derived from the MD simulation. The docking results are shown in Figure 9. It can be seen that these five ligands adopt the same orientation in the binding pocket. The pyrimidine rings of these ligands are almost overlapped and hydrogen bonded with T66 of the protein. Table I gives the binding energies and inhibition constants (*Ki*) calculated by docking and the corresponding experimental IC_{50}, which shows that the order of inhibitory activity calculated by docking is consistent with the experimental results [21]. These compounds showed a potency gain with

[1]The final structure of each AK system after MD simulation is derived from the average of the last 5 ns MD trajectory.

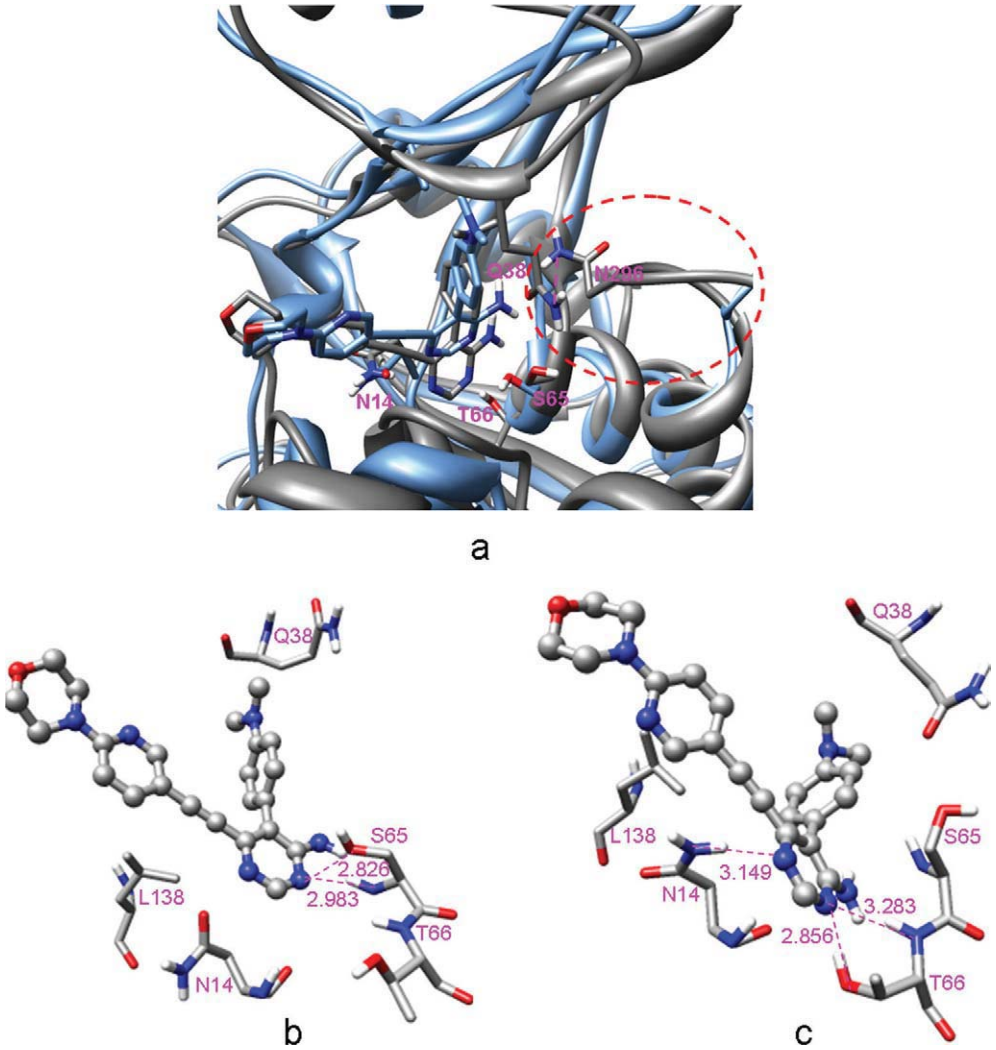

FIGURE 7. (a) Superposition of the docking structure (blue) and average structure derived from MD simulation (gray) of AK-APy complex. The red elliptical part represents residues 295-297, the same as below. (b) and (c) represent the different hydrogen bonds in docking structure and average structure obtained by MD simulation, respectively. [Color figure can be viewed in the online issue, which is available at wileyonlinelibrary.com.]

increasing the length of linker between the pyrimidine ring and phenyl group in which AP3 is the most potent inhibitor. But further extending the linker to four carbons such as AP4 will lead to the loss of potency. It can be explained by Figure 9 that when the linker increased from one to three carbons, the phenyl group could extend to the deeper hydrophobic pocket, the hydrophobic interaction between the ligand and AK increased. But when increased to four carbons, the longer chain linker made the phenyl group being close to the hydrophilic groups of D18, which decreased the interaction between the ligand and AK, therefore reduced inhibition constants.

3.2.2. Conformational Change of AK Complexed With AN

The superposition of AK-AN complex from the docking and the average structure derived from MD simulation is shown in Figure 10(a). After MD simulation, the small domain of AK underwent a rotation of 22° relative to the large domain. The backbone RMSD of AK is 2.5 Å, which is higher than that of AK-AN system. Meanwhile, there is coil-to-helix transition in residues 295–297 [the elliptical part in Fig. 10(a)].

Compared with the docking conformation, the side chain of N14 rotated and formed one H-bond with N3 atom of AN after MD simulation. With the

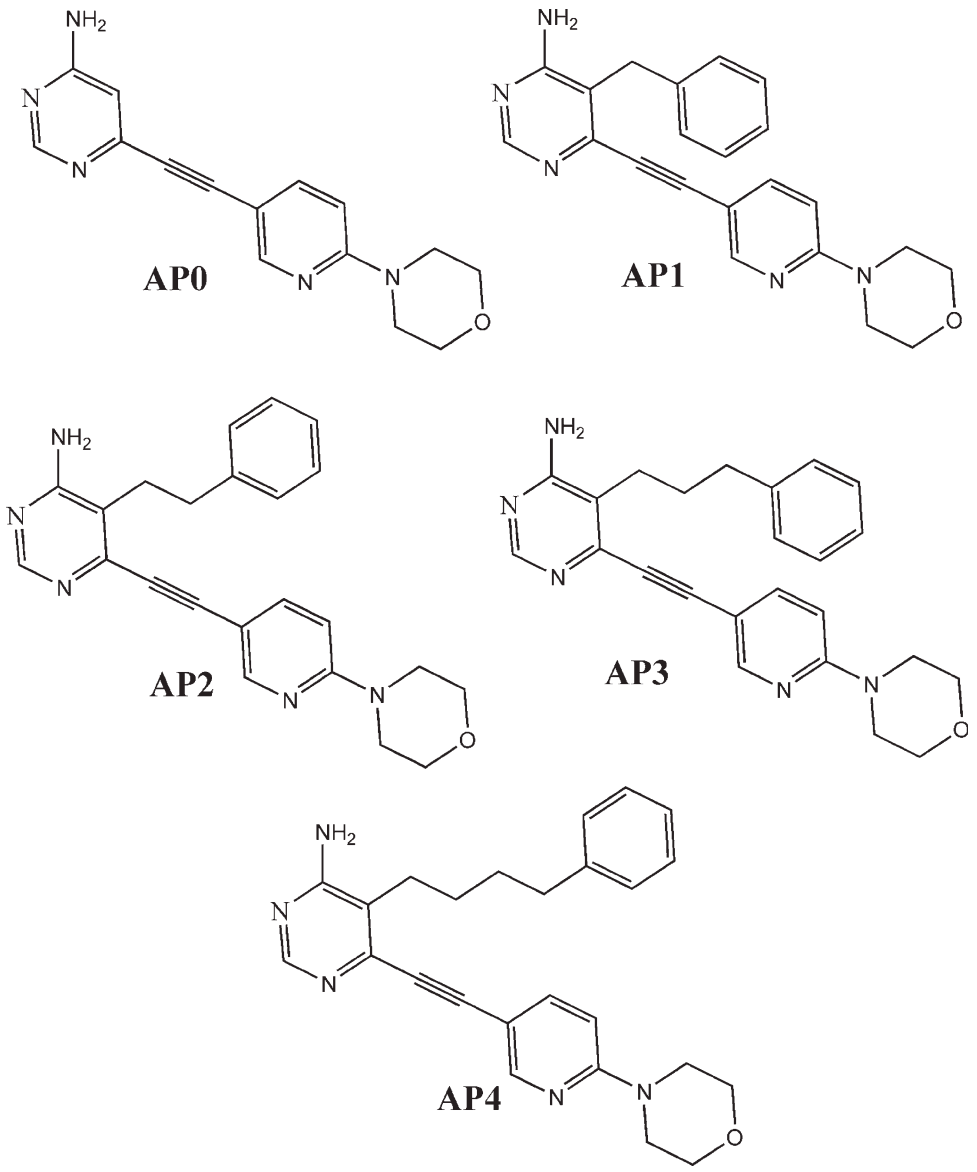

FIGURE 8. Structure of APy analogues, AP0, AP1, AP2, AP3, and AP4.

rotation of the small lid domain toward the large domain, the binding pocket reduced. However, because of the steric hindrance of large substitutions at C4 and C5 positions of AN, AK can not completely close and stabilize at a semiopen conformation.

During MD simulation, the purine ring of AN was steady in the binding pocket, but the sugar ring was mobile. This conclusion can be deduced from the distance fluctuation of several important H-bonds between the AN and the protein [Fig. 10(b)] and can be explained by two reasons: (i) In semiopen conformation, the bonding pocket is larger than that in closed structure, which provides spatial allowance for the rotation of the ligand's sugar ring. (ii) Comparing with the natural ligand ADO [22], AN has no hydroxyl at C5′ position and can not form H-bond with residue D300, which weaken the interaction between the protein and the sugar ring of AN.

Our MD simulation results of AK-AN complex agree well with the conclusion by Bhutoria and Ghoshal [30] that aryl nucleoside analogues can bind to semiopen conformation of human AK. However, for Bhutoria and Bhutoria, the semiopen conformation was homology modeled based on *T. gondii* AK (TAK) structure, and the rotation of the small domain was only 12°. In our research, the semiopen conformation of AK is obtained by

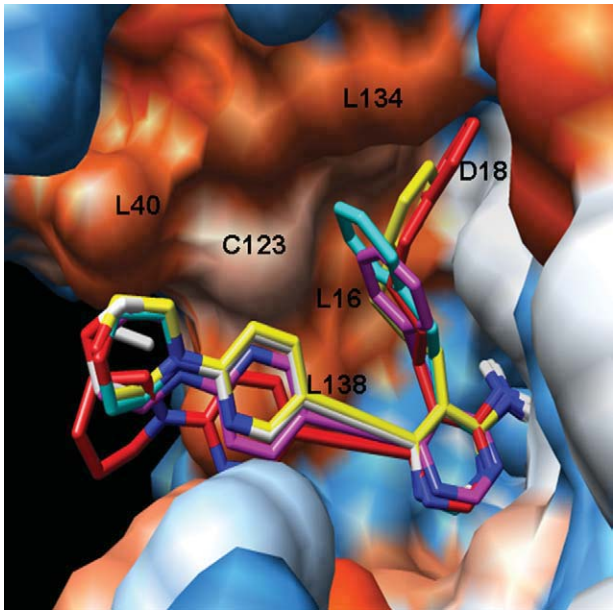

FIGURE 9. Superposition of the docking results of AP0-AP4 in the lipophilic potential surface constructed by surrounding residues (transect map), as color changes from red to blue, surface changes gradually from hydrophobic to hydrophilic. For the sake of distinguishing: white is for AP0, magenta for AP1, blue for AP2, yellow for AP3, and red for AP4. [Color figure can be viewed in the online issue, which is available at wileyonlinelibrary.com.]

MD simulation, which is more credible than that of homology models, and the rotation of the small domain is 22° relative to the large domain.

TABLE I

Binding energies and inhibition constants (*Ki*) of AK complexed with APy analogues and corresponding experimental IC_{50}.

Inhibitors	Binding energy (kcal/mol)	Inhibition constant, *Ki*, nM (298.15 K)	IC_{50} nM (298.15 K)[a]
AP0	−8.05	1270	120
AP1	−9.83	62.08	40
AP2	−10.47	21.08	4.5
AP3	−10.80	12.17	2.5
AP4	−10.38	24.70	38

[a] Assay with cytosolic AK from Ref. [21].

3.2.3. Kinetic Characteristic of 2I6B apo

The MD simulation of 2I6B apo shows that the system reaches equilibrium after the first 5 ns, and the RMSD maintains at 3.0 Å. An overlay of the average structure derived from MD simulation and the structure before MD is shown in Figure 11. For a better view, the closed crystal structure of AK (PDB code 2I6A) is also superposed in Figure 11. We found that after MD simulation, the structure of 2I6B apo changed and reached to the closed conformation. This agrees well with the experimental results [22, 29]. The MD average structure of 2I6B apo is quite coincident with the closed crystal structure (2I6A), which increases the reliability of our simulations.

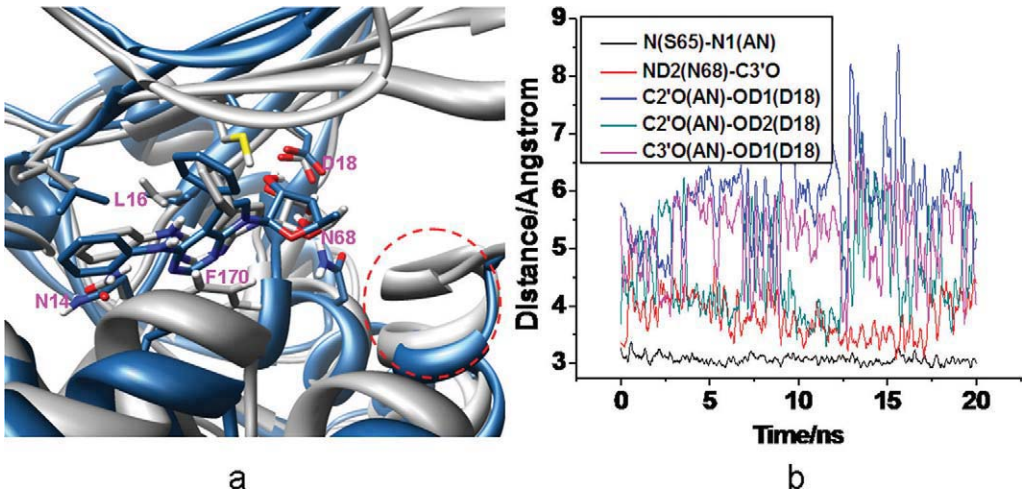

FIGURE 10. (a) Superposition of the docking structure (blue) and average structure derived from MD simulation (gray) of AK-AN complex. (b) Time courses of hydrogen bond lengths between AK and AN. [Color figure can be viewed in the online issue, which is available at wileyonlinelibrary.com.]

FIGURE 11. Superposition of the average structure derived from MD simulation (gray) and structure before MD (blue) of 2I6B apo, as well as the crystal structure of 2I6A (red). [Color figure can be viewed in the online issue, which is available at wileyonlinelibrary.com.]

Studies of both the apo and inhibited forms of TAK have revealed that apo form of TAK is in open conformation, which presumably allows for the initial binding of the substrate and the cofactor. On binding, the conformational switch G68-G69 is trigged, and the two domains rotate into the closed conformation in which the chemical reaction achieved [24]. For human AK, the crystal structure of apo has not been obtained. In the open conformation of 2I6B, the corresponding conformational switch G63-G64 has been "turned on" by ligand binding; therefore, 2I6B apo can rotate to the closed conformation after MD simulation. But, in AK-APy and AK-AN systems, with the steric hindrance of APy and AN, the lid domain can not completely close. According to the shapes of ligands, AK-APy and AK-AN systems can stabilize at different semiopen conformations after MD simulations.

4. Conclusion

Conformational rearrangement on binding natural substrate or inhibitors is a usual observation in protein structural studies [40], the implications of conformational change for structure-based drug design are significant. In this research, based on the crystal structure of open conformation of AK, we performed the docking and MD simulations to study the conformational changes induced by inhibitors APy and AN. The MD simulations results indicate that APy and AN can induce different conformational changes of AK. For AK-APy system, the small lid domain of AK rotated 14° and then stabilized at a semiopen conformation. Furthermore, the binding pocket of APy rearranged. Docking studies of APy analogues proved the structural rationality of this semiopen conformation. For AK-AN system, the rotation of the small domain was 22°, and the MD simulation showed only minor change in the binding pocket, but the sugar ring of AN was mobile during simulation.

References

1. Ralevic, V.; Burnstock, G. Pharmacol Rev 1998, 50, 413.
2. Williams, M.; Jarvis, M. F. Biochem Pharmacol 2000, 59, 1173.
3. Moser, G. H.; Schrader, J.; Deussen, A. Am J Physiol 1989, 256, C799.
4. Arch, J. R.; Newsholme, E. A. Biochem J 1978, 174, 965.
5. Griffith, D. A.; Jarvis, S. M. Biochim Biophys Acta 1996, 1284, 213.
6. Golembiowska, K.; White, T. D.; Sawynok, J. Brain Res 1995, 699, 315.
7. Kowaluk, E. A.; Jarvis, M. F. Expert Opin Investig Drugs 2000, 9, 551.
8. Kowaluk, E. A.; Mikusa, J.; Wismer, C. T.; Zhu, C. Z.; Schweitzer, E.; Lynch, J. J.; Lee, C. H.; Jiang, M. Q.; Bhagwat, S. S.; Gomtsyan, A.; McKie, J.; Cox, B. F.; Polakowski, J.; Reinhart, G.; Williams, M.; Jarvis, M. F. J Pharmacol Exp Ther 2000, 295, 1165.
9. Williams, M.; Kowaluk, E. A.; Arneric, S. P. J Med Chem 1999, 42, 1481.
10. Kowaluk, E. A.; Kohlhaas, K. L.; Bannon, A.; Gunther, K.; Lynch, J. J.; Jarvis, M. F. Pharmacol Biochem Behav 1999, 63, 83.
11. Wiesner, J. B.; Ugarkar, B. G.; Castellino, A. J.; Barankiewicz, J.; Dumas, D. P.; Gruber, H. E.; Foster, A. C.; Erion, M. D. J Pharmacol Exp Ther 1999, 289, 1669.
12. Bennett, L. L.; Hill, D. L. Mol Pharmacol 1975, 11, 803.
13. Davies, L. P.; Jamieson, D. D.; Baird-Lambert, J. A.; Kazlauska, R. Biochem Pharmacol 1984, 33, 347.
14. Kubo, I.; Kim, M.; Wood, W. F.; Naoki, H. Tetrahedron Lett 1986, 27, 4277.
15. Erion, M. D.; Rydzewski, R. M. Nucleos Nucleot Nucleic Acids 1997, 16, 315.

16. Perner, R. J.; Lee, C. H.; Jiang, M. Q.; Gu, Y. G.; DiDomenico, S.; Bayburt, E. K.; Alexander, K. M.; Kohlhaas, K. L.; Jarvis, M. F.; Kowaluk, E. L.; Bhagwat, S. S. Bioorg Med Chem Lett 2005, 15, 2803.
17. Matulenko, M. A.; Paight, E. S.; Frey, R. R.; Gomtsyan, A.; DiDomenico, S.; Jiang, M.; Lee, C. H.; Stewart, A. O.; Yu, H.; Kohlhaas, K. L.; Alexander, K. M.; McGaraughty, S.; Mikusa, J.; Marsh, K. C.; Muchmore, S. W.; Jakob, C. L.; Kowaluk, E. A.; Jarvis, M. F.; Bhagwat, S. S. Bioorg Med Chem Lett 2007, 15, 1586.
18. Zheng, G. Z.; Lee, C. H.; Pratt, J. K.; Perner, R. J.; Jiang, M. Q.; Gomtsyan, A.; Matulenko, M. A.; Mao, Y.; Koenig, J. R.; Kim, K. H.; Muchmore, S.; Yu, H. X.; Kohlhaas, K.; Alexander, K. M.; McGaraughty, S.; Chu, K. L.; Wismer, C. T.; Mikusa, J.; Jarvis, M. F.; Marsh, K.; Kowaluk, E. A.; Bhagwat, S. S.; Stewart, A. O. Bioorg Med Chem Lett 2001, 11, 2071.
19. Lee, C. H.; Jiang, M. Q.; Cowart, M.; Gfesser, G.; Perner, R.; Kim, K. H.; Gu, Y. G.; Williams, M.; Jarvis, M. F.; Kowaluk, E. A.; Stewart, A. O.; Bhagwat, S. S. J Med Chem 2001, 44, 2133.
20. Gomtsyan, A.; Didomenico, S.; Lee, C. H.; Stewart, A. O.; Bhagwat, S. S.; Kowaluk, E. A.; Jarvis, M. F. Bioorg Med Chem Lett 2004, 14, 4165.
21. Gomtsyan, A.; Didomenico, S.; Lee, C. H.; Matulenko, M. A.; Kim, K.; Kowaluk, E. A.; Wismer, C. T.; Mikusa, J.; Yu, H. X.; Kohlhaas, K.; Jarvis, M. F.; Bhagwat, S. S. J Med Chem 2002, 45, 3639.
22. Mathews, I. I.; Erion, M. D.; Ealick, S. E. Biochemistry 1998, 37, 15607.
23. Cook, W. J.; DeLucas, L. J.; Chattopadhyay, D. Protein Sci 2000, 9, 704.
24. Schumacher, M. A.; Scott, D. M.; Mathews, I. I.; Ealick, S. E.; Roos, D. S.; Ullman, B.; Brennan, R. G. J Mol Bio 2000, 298, 875.
25. Zhang, Y.; el Kouni, M. H.; Ealick, S. E. Acta Cryst 2007, D63, 126.
26. Reddy, M. C. M.; Palaninathan, S. K.; Shetty, N. D.; Owen, J. L.; Watson, M. D.; Sacchettini, J. C. J Biol Chem 2007, 282, 27334.
27. Zhu, R. X.; Zhang, X. L.; Dong, X. C.; Chen, M. B. Chinese J Chem 2006, 24, 1493.
28. Lee, Y.; Bharatham, N.; Bharatham, K.; Lee, K. W. Bull Kor Chem Soc 2007, 28, 561.
29. Muchmore, S. W.; Smith, R. A.; Stewart, A. O.; Cowart, M. D.; Gomtsyan, A.; Matulenko, M. A.; Yu, H. X.; Severin, J. M.; Bhagwat, S. S.; Lee, C. H.; Kowaluk, E. A.; Jarvis, M. F.; Jakob, C. L. J Med Chem 2006, 49, 6726.
30. Bhutoria, S.; Ghoshal, N. J Mol Graph Model 2010, 28, 577.
31. Ugarkar, B. G.; Castellino, A. J.; DaRe, J. M.; Kopcho, J. J.; Wiesner, J. B.; Schanzer, J. M.; Erion, M. D. J Med Chem 2000, 43, 2894.
32. Frisch, M. J.; Trucks, G. W.; Schlegel, H. B.; Scuseria, G. E.; Robb, M. A.; Cheeseman, J. R.; Montgomery, J. A., Jr.; Vreven, T.; Kudin, K. N.; Burant, J. C.; Millam, J. M.; Iyengar, S. S.; Tomasi, J.; Barone, V.; Mennucci, B.; Cossi, M.; Scalmani, G.; Rega, N.; Petersson, G. A.; Nakatsuji, H.; Hada, M.; Ehara, M.; Toyota, K.; Fukuda, R.; Hasegawa, J.; Ishida, M.; Nakajima, T.; Honda, Y.; Kitao, O.; Nakai, H.; Klene, M.; Li, X.; Knox, J. E.; Hratchian, H. P.; Cross, J. B.; Bakken, V.; Adamo, C.; Jaramillo, J.; Gomperts, R.; Stratmann, R. E.; Yazyev, O.; Austin, A. J.; Cammi, R.; Pomelli, C.; Ochterski, J. W.; Ayala, P. Y.; Morokuma, K.; Voth, G. A.; Salvador, P.; Dannenberg, J. J.; Zakrzewski, V. G.; Dapprich, S.; Daniels, A. D.; Strain, M. C.; Farkas, O.; Malick, D. K.; Rabuck, A. D.; Raghavachari, K.; Foresman, J. B.; Ortiz, J. V.; Cui, Q.; Baboul, A. G.; Clifford, S.; Cioslowski, J.; Stefanov, B. B.; Liu, G.; Liashenko, A.; Piskorz, P.; Komaromi, I.; Martin, R. L.; Fox, D. J.; Keith, T.; Al-Laham, M. A.; Peng, C. Y.; Nanayakkara, A.; Challacombe, M.; Gill, P. M. W.; Johnson, B.; Chen, W.; Wong, M. W.; Gonzalez, C.; Pople, J. A. Gaussian 03, Revision C. 02; Gaussian, Inc.: Wallingford, CT, 2004.
33. Morris, G. M.; Goodsell, D. S.; Halliday, R. S.; Huey, R.; Hart, W. E.; Belew, R. K.; Olson, A. J. J Comput Chem 1998, 19, 1639.
34. Sanner, M. F. J Mol Graph Model 1999, 17, 57.
35. Lindahl, E.; Hess, B.; van der Spoel, D. J Mol Model 2001, 7, 306.
36. Schuttelkopf, A. W.; van Aalten, D. M. F. Acta Cryst 2004, D60, 1355.
37. Wlodek, S. T.; Clark, T. W.; Scott, L. R.; McCammon, J. A. J Am Chem Soc 1997, 119, 9513.
38. Hayward, S.; Berendsen, H. J. C. Protein Struct Funct Genet 1998, 30, 144.
39. Hayward, S.; Lee, R. A. J Mol Graph Model 2002, 21, 181.
40. Gutteridge, A.; Thornton, J. J Mol Biol 2005, 346, 21.